An analysis of the NREL 5 MW semisubmersible wind turbine using data from Morro Bay

By

Ayush Kumar Singh, Kenneth Anthony Dmello, Gaurav Ashwin Chandavarkar

Introduction:

This project intends to first cover the potential for offshore wind energy in the United States and compare it with the rest of the world. The second section covers some of the basic installations of offshore wind turbines including fixed and floating and then moves onto the analysis which was done using QBlade. Using offshore wind turbines comes with a host of advantages. There are no physical restrictions such as hills or buildings that could block the wind flow. Offshore wind speeds tend to be steadier than on land and more directionally consistent. Being miles out from the coast, offshore turbines are further away from the local population. Restricted access to their sites may even help to protect the surrounding marine ecosystems. A half of the population of the United States lives in coastal areas. Large offshore wind turbines suffer high extreme loads due to their size; in addition, the lack of noise restrictions allow higher tip speeds. Consequently, the airfoils presented in this work are designed for high Reynolds numbers with the main goal of reducing blade loads and maintaining power production. Oceans provide the perfect location to build wind farms in terms of scale and openness. More wind farms being built means more clean, sustainable energy can be produced. The adoption of wind energy can encourage investment in other renewable sources which can be used in conjunction with wind energy. DOE Wind Vision estimated between 76000-80000 jobs can be created with wind energy. The UK has invested significantly into the building and commissioning of a 1.3GW capacity wind farm called Hornsea Phase 2 which became operational in August 2022.

Fig.1. Hornsea Phase 2 uses 165 8MW turbines with a combined capacity of 1.3GW

Offshore potential in the United States:

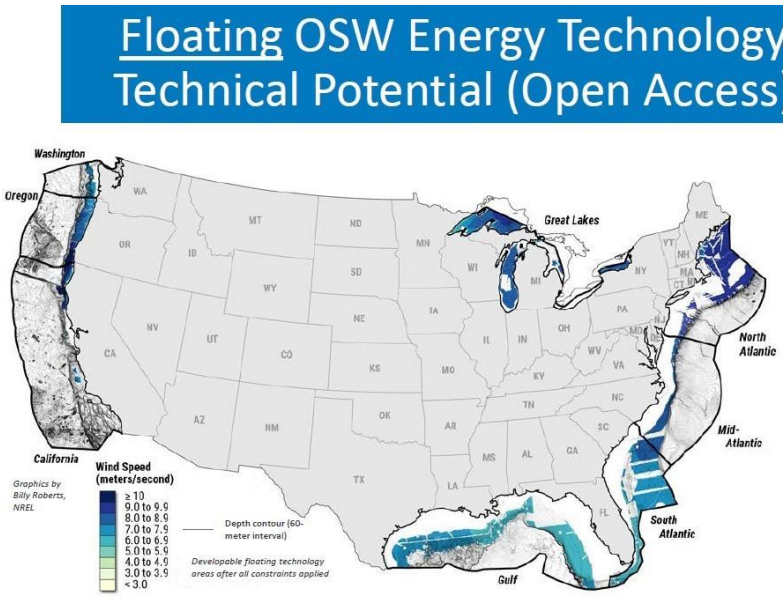

Region	GW	TWh
California	88	338
Great Lakes	415	1,535
Gulf	867	2,289
Mid Atlantic	166	607
North Atlantic	442	1,843
Oregon	150	544
South Atlantic	586	1,628
Washington	59	188
CONUS Total	**2,773**	**8,972**

*values are rounded to closest integer

Fig. 2. Floating OSW capacity comes to 2773GW with Gulf and Atlantic regions showing the highest potential

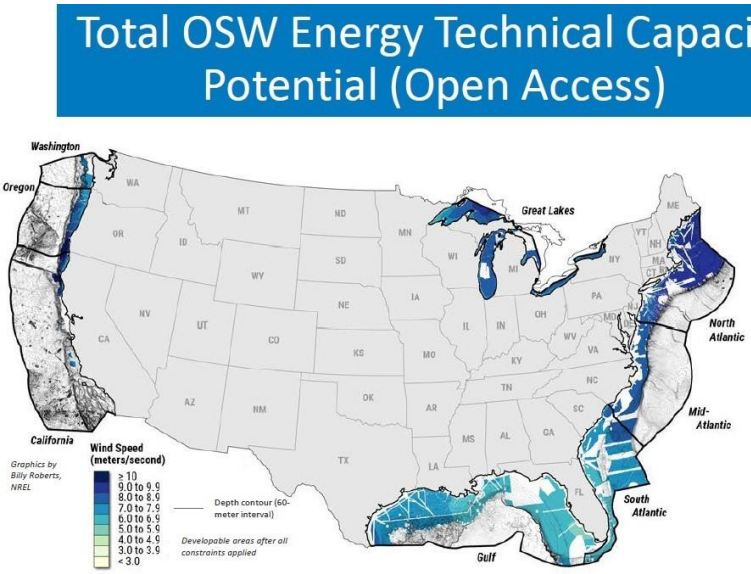

Region	Fixed-Bottom (GW)	Floating (GW)	Fixed-Bottom (%)	Floating (%)
California	4	88	4	96
Great Lakes	160	415	28	72
Gulf	696	867	45	55
Mid-Atlantic	157	166	49	51
North Atlantic	264	442	37	63
Oregon	2	150	1	99
South Atlantic	188	586	24	76
Washington	5	59	8	92
CONUS Total	**1,476**	**2,773**	35	65

*values are rounded to closest integer

Note: DOD-defined wind exclusion areas constitute an area equivalent to an additional 428 GW of California OSW wind energy potential.

NREL | 16

Fig. 3.Total OSW capacity comes to 4249 GW with Gulf and Atlantic regions showing the highest potential

In the United States, OSW energy is at a more nascent stage with only seven turbines, totaling 42 megawatts (MW), installed through 2021. Over 40 gigawatts (GW) of OSW energy capacity are at various stages of development as of 2021. Eighteen projects in the U.S. offshore pipeline have reached the permitting phase, and eight states have set their own offshore wind energy procurement goals, which total 40 GW by 2040.

European investment in offshore:

FIGURE 18
New offshore wind investments and capacity financed: 2010 – 2020 (€bn)

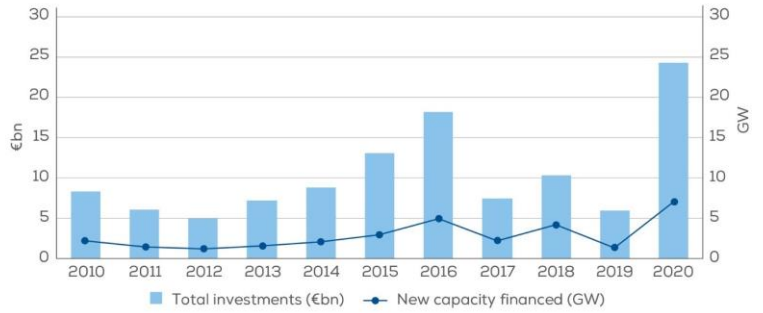

	2010	2011	2012	2013	2014	2015	2016	2017	2018	2019	2020
Total investments (€bn)	8.4	6.1	5	7.2	8.8	13.1	18.2	7.5	10.3	6	24.2
New capacity financed (GW)	2.2	1.5	1.3	1.6	2.1	3	5	2.3	4.2	1.4	7.1

Source: WindEurope

Fig. 4. Investments in Europe over a 10-year period

Currently, the EU is a global leader in the manufacturing of key wind turbine components, as well as in the foundations and cables industry: almost half of the active companies in the wind sector (onshore and offshore) are headquartered in the EU. To explore offshore sites further out to sea with stronger and more consistent winds, several European developers are working on floating offshore wind turbines. Multiple pilot projects are already up and running, with deployment expected to accelerate towards the end of this decade. The deployment of offshore wind energy is at the core of delivering the European Green Deal. The installed offshore wind capacity in the EU was 14.6 GW in 2021 and is set to increase by at least 25 times by 2030, using the vast potential of the 5 EU sea basins. The strategy sets targets for an installed capacity of at least 60 GW of offshore wind by 2030, and 300 GW by 2050. Europe now has a total installed offshore wind capacity of 25 GW. That corresponds to 5,402 grid-connected wind turbines across 12 countries. Europe added 2.9 GW of offshore capacity during 2020. That's 356 new offshore wind turbines connected to the grid, across nine wind farms. Investments in new assets accounted for €26.3bn in order to finance 7.1 GW of additional capacity.

Types of Offshore installations:

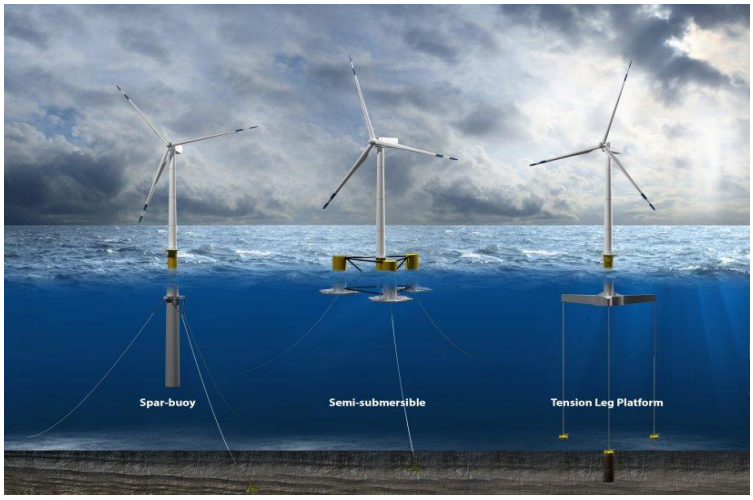

Fig. 5. Floating type turbine installations

- **Spar :** This type achieves system stability with the help of ballast installed below the main buoyancy tank to maintain a proper centre of buoyancy.
- **Semisubmersible :** Achieves static stability by distributing buoyancy widely at the water surface level. Easier to transport and setup at site.
- **Tension Leg Platform:** Stability is achieved by mooring lines attached to a submerged buoyancy tank

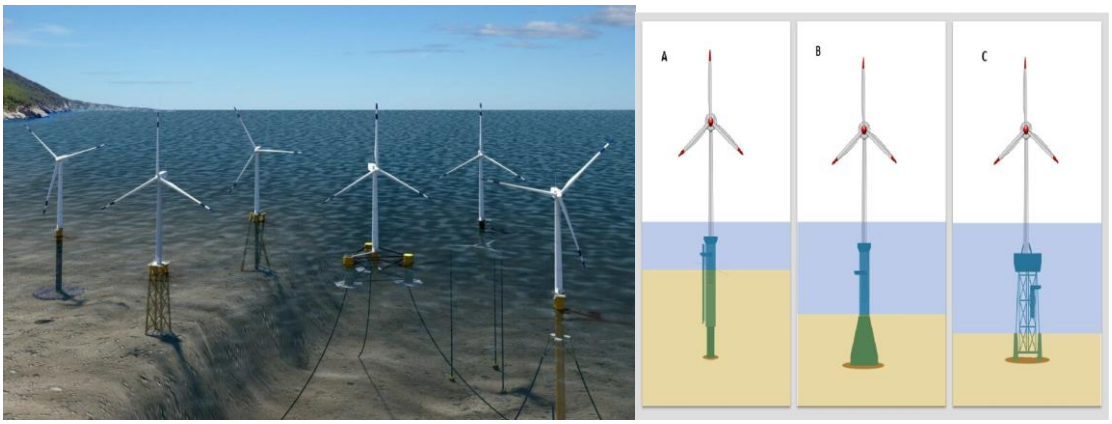

Fig. 5. From L-R: Gravity based, Jacket, Tripod, Semisubmersible, Tension Leg Platform, Spar-buoy

- **Monopile Foundations(A):** Can be used to depths to 40 m. They are a common choice for offshore turbines located in shallow water (less than 35 m). Cost-effective for installations to 40 m. Have a simple design that installs quickly.

- **Gravity-Based Foundations(B):** Suitable for sites to depths up to 30 m. Some designs do not need crane installation. Tugboats can move port-assembled floated-to-fixed GBFs into place, reducing costs and risk.
- **Jacket Foundations(C):** Can be installed to depths of 60 m. Can be installed using piles or suction caissons in stiff clays or medium-to-dense sands. Economical choice using straightforward manufacturing methods.

Airfoil:

Wind turbine blades use airfoils to develop mechanical power. The cross-sections of wind turbine blades have the shape of airfoils. The flow velocity over airfoils increases over the convex surface resulting in lower average pressure on the 'suction' side of the airfoil compared with the concave or 'pressure' side of the airfoil.

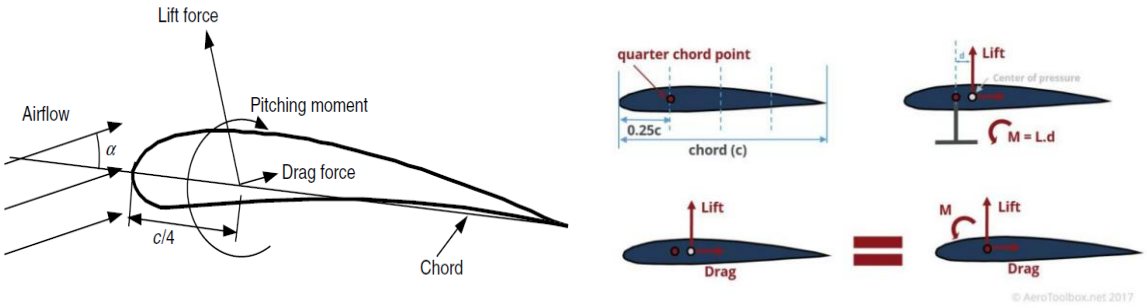

The resultant of all of these pressure and friction forces is usually resolved into two forces and a moment that act along the chord at a distance of c=4 from the leading edge (at the 'quarter chord').

Center of Pressure

The net vertical force is termed the lifting force and the net horizontal force is termed the drag force. The net lift and drag force acts at the center of pressure of the airfoil. However, the center of pressure is not a fixed point and will vary as the angle of attack of the airfoil is varied.

Quarter Chord

The center of pressure is therefore not a convenient location about which to specify the resultant forces acting on the airfoil as it is not fixed. A common convention is to use a point

specified at the airfoil quarter chord. This is a point located one quarter of the way along the chord from the leading edge. Moving the resultant lift and drag force from the center of pressure to the quarter chord requires that a moment be added to achieve a force balance. Thus a pitching moment equal to the lift force multiplied by the moment arm between the quarter chord and the center of pressure is added to achieve static equilibrium (Here we have neglected the component of the shear force that would contribute to the total pitching moment as it is negligibly small relative to the lift component).

At angles of attack below around ten to fifteen degrees, the lift increases with an increasing angle. However, if the angle of attack is too large, stalling takes place. Stalling occurs when the lift decreases, sometimes very suddenly. The phenomena responsible for stalling is flow separation (see Figure 9). Flow separation is the situation where the fluid flow no longer follows the contour of the wing surface. Fluid particles flowing along the top of the wing surface experience a change in pressure, moving from the ambient pressure in front of the wing, to a lower pressure over the surface of the wing, then back up to the ambient pressure behind the wing. The region where fluid must flow from low to high pressure (adverse pressure gradient) is responsible for flow separation. If the pressure gradient is too high, the pressure forces overcome the fluid's inertial forces, and the flow departs from the wing contour. Since the pressure gradient increases with an increasing angle of attack, the angle of attack should not exceed the maximum value to keep the flow following the contour. If this angle is exceeded, however, the force keeping the plane in the air will decrease, and may even disappear altogether.

$$C_l = \frac{L/l}{\frac{1}{2}\rho U^2 c} = \frac{\text{Lift force/unit length}}{\text{Dynamic force/unit length}}$$

Two-dimensional Lift coefficient

$$C_d = \frac{D/l}{\frac{1}{2}\rho U^2 c} = \frac{\text{Drag force/unit length}}{\text{Dynamic force/unit length}}$$

Two-dimensional Drag coefficient

$$C_m = \frac{M}{\frac{1}{2}\rho U^2 A c} = \frac{\text{Pitching moment}}{\text{Dynamic moment}}$$

Pitching moment coefficient

NACA 4-digit airfoil specification

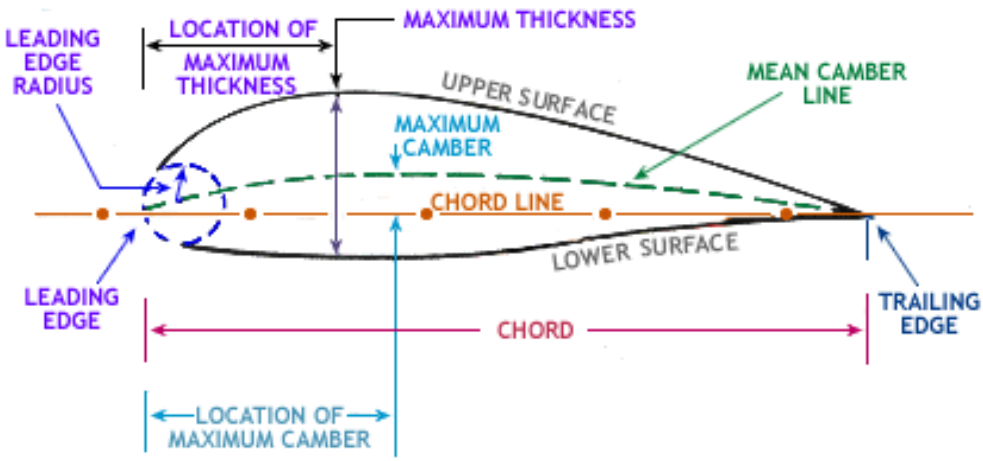

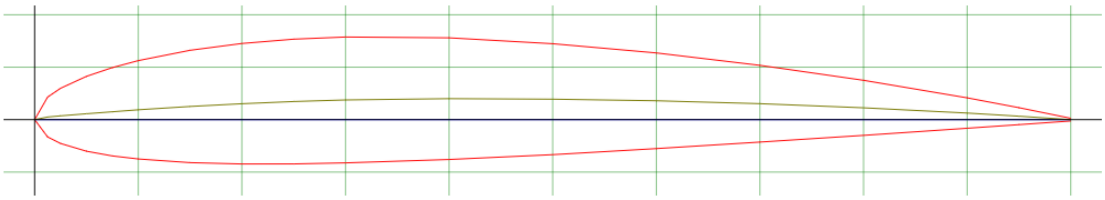

This NACA airfoil series is controlled by 4 digits e.g. NACA 2412, which designate the camber, position of the maximum camber and thickness. If an airfoil number is

NACA MPXX

NACA 2412

- M is the maximum camber divided by 100. In the example M=2 so the camber is 0.02 or 2% of the chord
- P is the position of the maximum camber divided by 10. In the example P=4 so the maximum camber is at 0.4 or 40% of the chord.
- XX is the thickness divided by 100. In the example XX=12 so the thickness is 0.12 or 12% of the chord.

Blade Twist

Because of lift differential due to differing rotational relative wind values along the blade, the blade should be designed with a twist to alleviate internal blade stress and distribute the lifting force more evenly along the blade. Blade twist provides higher pitch angles at the root where velocity is low and lower pitch angles nearer the tip where velocity is higher. This increases the induced air velocity and blade loading near the inboard section of the blade.

Data processing:

The data we used was obtained from the LiDAR buoy stationed at Morro Bay which used a host of sensors to measure and collect wind speed, direction, GPS, time, water depth and sea salinity data. Data processing was done to extract velocity data from NetCDF files using a modified version of VAD code to calculate mean velocities for each range ring which ranged from 40m to 250m above sea surface. The data was extracted for 457 days starting in October 2020. This velocity was used to evaluate the BEM model as explained below.

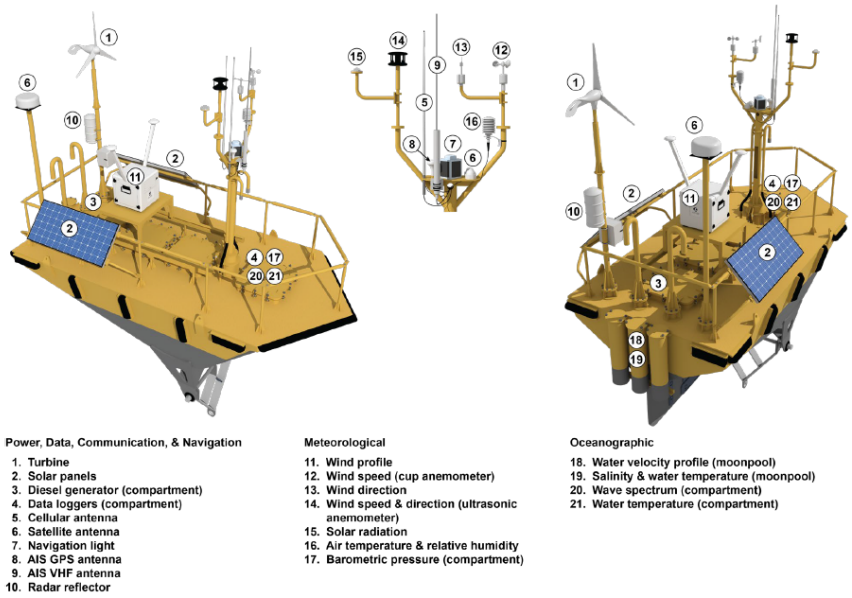

Fig. 6. LIDAR buoy equipped with anemometers, antennae, and other sensors

max_velocity.m | code_final.m | data_extract.m | new_file.m

```
vars_to_load =  {'wind_speed', 'wind_direction', 'time'};
projectdir = '/MATLAB Drive/Wind Energy/Project';
info = dir( fullfile(projectdir, '*.nc') );
n_files = length(info);
filenames = fullfile( projectdir, {info.name} );
lat = cell(n_files,1);
lon = cell(n_files,1);
series = cell(n_files, 1);
time= cell(n_files,1);
for k = 1 : n_files
  f = filenames{k};
  wind_velocity{k} = ncread(f, vars_to_load{1});
  wind_direction{k} = ncread(f, vars_to_load{2});
  time{k} = ncread(f, vars_to_load{3});
end
```

max_velocity.m | code_final.m | data_extract.m | new_file.m

```
%z=zeros(12,457);
for q=1:457
    for n=1:12
        p=wind_velocity{1,q};
        p(isnan(p))=0;
        w(n,q)=max(p(n,:));


    end
end
for q=1:457
    for n=1:12
        rc=find(wind_velocity{1,q}(n,:)==w(n,q));
%         z(n,q)=wind_direction{1,q}(n,rc);
    end
end
final_mean = mean(w,2);
```

Fig. 7. MATLAB code to extract velocity and calculate mean velocities.

Height (m)	Average Windspeed (m/s)
40	12.8472
56.67	13.4042
73.4	13.9984
90.01	14.242
106.68	14.491
123.35	15.0871
140.02	15.7491
156.69	16.4324
173.36	17.2114
190.03	17.9142
206.67	18.3965
223.37	16.6033

Fig. 7. Mean velocities for all range gates.

Characteristics of 5MW turbine

We used the NREL 5MW turbine as our reference turbine for analysis at Morro Bay. The semisubmersible installation was chosen given the depth of water at site (190m) and the advantages of the mounting such as cost of assembly and ease of installation. Given below are the characteristics of the turbine as provided by NREL.

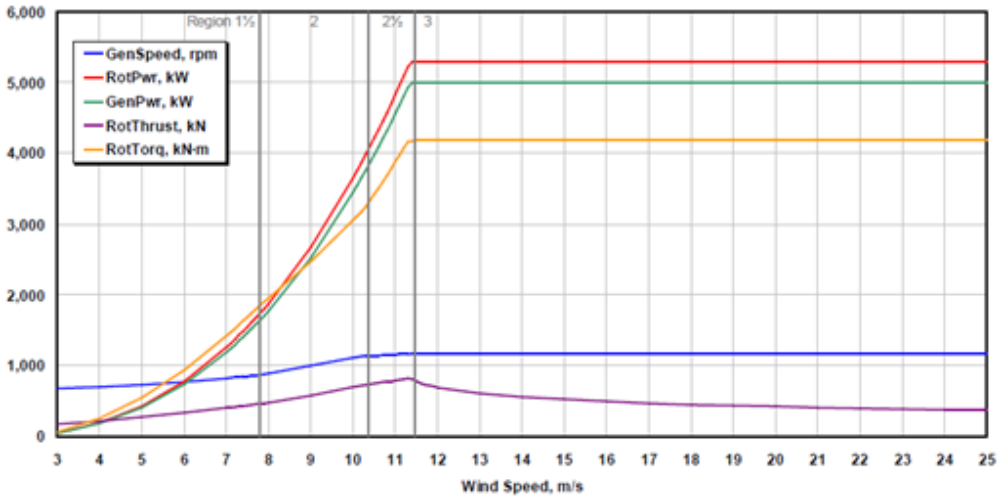

Fig. 8. Power, torque and thrust characteristics of NREL 5MW turbine.

Node	RNodes(m)	AeroTwst(º)	DRNodes (m)	Chord(m)	Airfoil Table
1	2.8667	13.308	2.7333	3.542	Cylinder1.dat
2	5.6000	13.308	2.7333	3.854	Cylinder1.dat
3	8.3333	13.308	2.7333	4.167	Cylinder2.dat
4	11.7500	13.308	4.1000	4.557	DU40_A17.dat
5	15.8500	11.480	4.1000	4.652	DU35_A17.dat
6	19.9500	10.162	4.1000	4.458	DU35_A17.dat
7	24.0500	9.011	4.1000	4.249	DU30_A17.dat
8	28.1500	7.795	4.1000	4.007	DU25_A17.dat
9	32.2500	6.544	4.1000	3.748	DU25_A17.dat
10	36.3500	5.361	4.1000	3.502	DU21_A17.dat
11	40.4500	4.188	4.1000	3.256	DU21_A17.dat
12	44.5500	3.125	4.1000	3.010	NACA64_A17.dat
13	48.6500	2.319	4.1000	2.764	NACA64_A17.dat
14	52.7500	1.526	4.1000	2.518	NACA64_A17.dat
15	56.1667	0.863	2.7333	2.313	NACA64_A17.dat
16	58.9000	0.370	2.7333	2.086	NACA64_A17.dat
17	61.6333	0.106	2.7333	1.419	NACA64_A17.dat

The table above gives the aerodynamic dimensions of the airfoil for the blade.

Given below is the list of parameters taken into account while modelling for the BEM analysis with hub height, rated capacity, rotor diameter, cut-in and cut-out speeds being the most important.

Rating	5 MW
Rotor Orientation, Configuration	Upwind, 3 Blades
Control	Variable Speed, Collective Pitch
Drivetrain	High Speed, Multiple-Stage Gearbox
Rotor, Hub Diameter	126 m, 3 m
Hub Height	90 m
Cut-In, Rated, Cut-Out Wind Speed	3 m/s, 11.4 m/s, 25 m/s
Cut-In, Rated Rotor Speed	6.9 rpm, 12.1 rpm
Rated Tip Speed	80 m/s
Overhang, Shaft Tilt, Precone	5 m, 5^{o}, 2.5^{o}
Rotor Mass	110,000 kg
Nacelle Mass	240,000 kg
Tower Mass	347,460 kg
Coordinate Location of Overall CM	(-0.2 m, 0.0 m, 64.0 m)

QBlade:

The software we selected to run our model using BEM was QBlade. It is a highly advanced multi-physics code that covers the complete range of aspects required for the aero-servo-hydro-elastic design, prototyping, simulation, and certification of wind turbines. It uses BEM (Blade Element Momentum Theory) to run simulations on various wind turbines.

The aerodynamics module to design blade and perform XFoil analysis by accounting for range of Angle of attack and Reynolds number.

There are three types of BEM modelling in QBlade:

- Rotor BEM: Modelling for aerodynamic outputs (Power and thrust coefficient) of blade profile

- Characteristic BEM: Modelling to predict power, thrust and torque output and using a given pitch range to optimise control characteristics
- Turbine BEM: Modelling power and thrust output accounting for rated capacity, transmission type and losses.

Airfoil sections:

We decided on using the DTU profiles DU40, DU30, DU25, DU21 and NACA64 to conduct an aerodynamic analysis using the mean wind velocity derived from the Morro Bay data. The above mentioned profiles were selected given their optimal lift characteristics especially in the primary and tip section over the given range of angle of attack. Given below are plots showing twist and chord variation over radius as well as profiles.

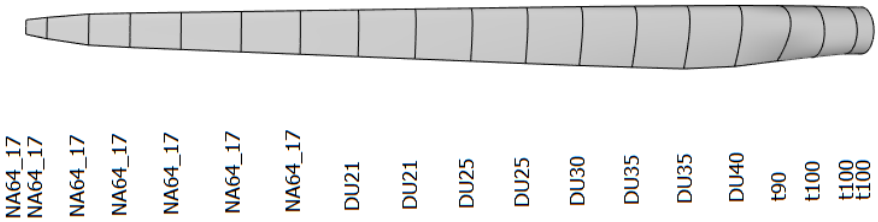

Fig. 9. Airfoil sections

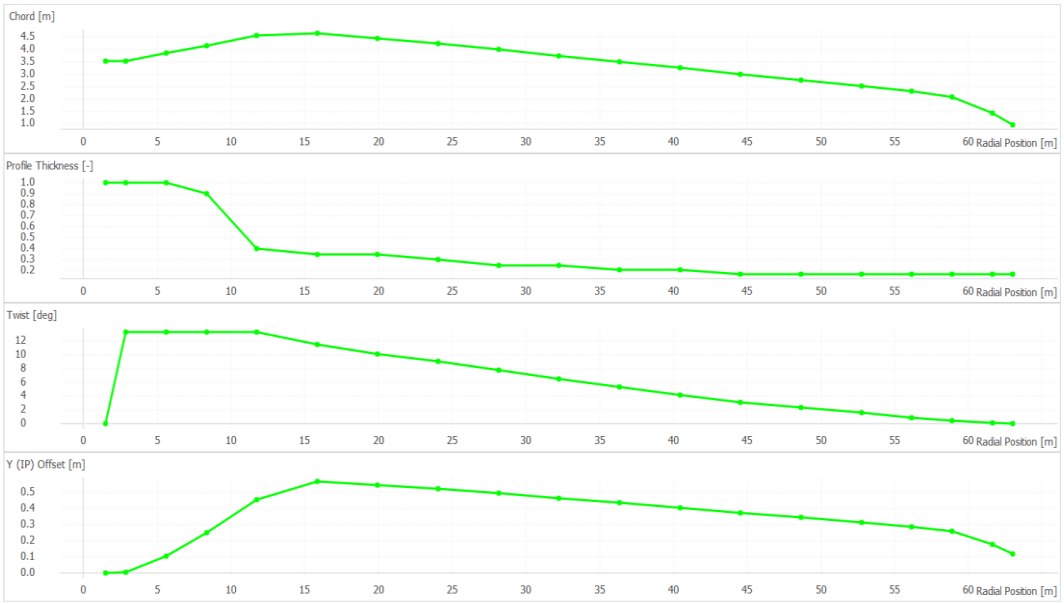

Fig. 10. Variation of chord, thickness, and twist over radius

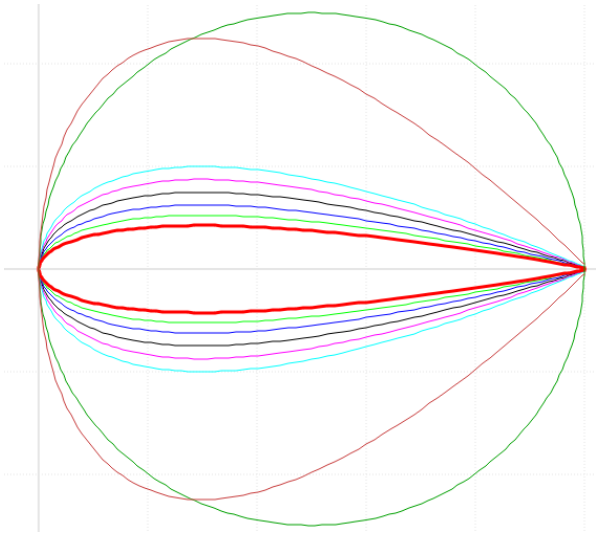

Airfoil analysis:

This module uses the X-Foil plug in to perform analysis at the Re number 937847 which was calculated from the mean velocity and by assuming constants such as air density, kinematic and dynamic density.

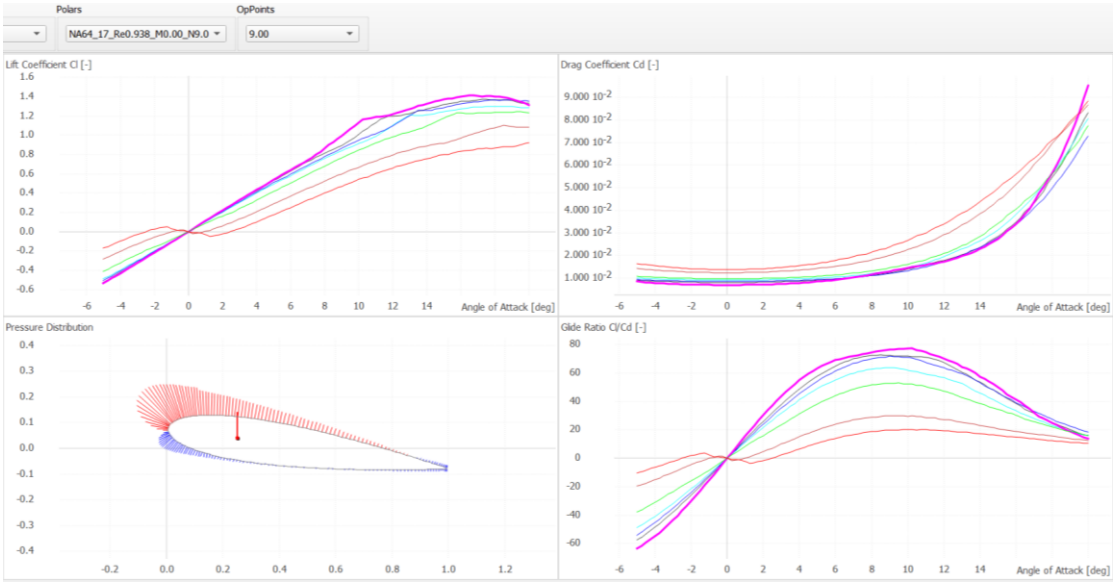

The graph above shows the variation of the lift and drag coefficients for all airfoil profiles over angles of attack ranging from -5 to 20°. It is observed NACA64_17 gives the best Cl, Cd and pressure distribution characteristics and justifies its choosing to model a significant portion of the airfoil. Given below is a sample of the table for Cl for various airfoil profiles.

	DU21_Re0.938_M0.00_N9.0	DU25_Re0.938_M0.00_N9.0	DU35_Re0.938_M0.00_N9.0	NA64_17_Re0.938_M0.00_N9.0
Angle of Attack	Cl	Cl	Cl	Cl
-5.000	-0.528	-0.491	-0.285	-0.537
-4.750	-0.502	-0.469	-0.265	-0.511
-4.500	-0.476	-0.446	-0.246	-0.485
-4.000	-0.424	-0.422	-0.225	-0.458
-3.750	-0.398	-0.399	-0.205	-0.432
-3.500	-0.372	-0.350	-0.187	-0.405
-3.250	-0.346	-0.326	-0.167	-0.379
-3.000	-0.319	-0.301	-0.147	-0.352
-2.750	-0.293	-0.276	-0.130	-0.325
-2.500	-0.267	-0.251	-0.110	-0.298
-2.250	-0.240	-0.227	-0.092	-0.271
-2.000	-0.213	-0.201	-0.076	-0.244
-1.750	-0.187	-0.177	-0.058	-0.217
-1.500	-0.161	-0.152	-0.042	-0.190
-1.250	-0.134	-0.126	-0.028	-0.163
-1.000	-0.107	-0.101	-0.014	-0.136
-0.750	-0.080	-0.076	-0.001	-0.109
-0.500	-0.053	-0.051	0.009	-0.082
-0.250	-0.027	-0.026	0.015	-0.054
0.000	0.000	0.000	0.020	-0.027
0.250	0.027	0.026	0.000	0.000
0.500	0.053	0.050	-0.021	0.027

Rotor BEM:

This model uses tip speed ratio as its input and in this case the range was set between 5-8^{o} as literature states this range is most optimal for designing offshore wind turbines as they tend to be larger. The graphs show the variation of power and thrust coefficients with respect to tip speed ratio as well as angle of attack and axial induction factor v/s radius.

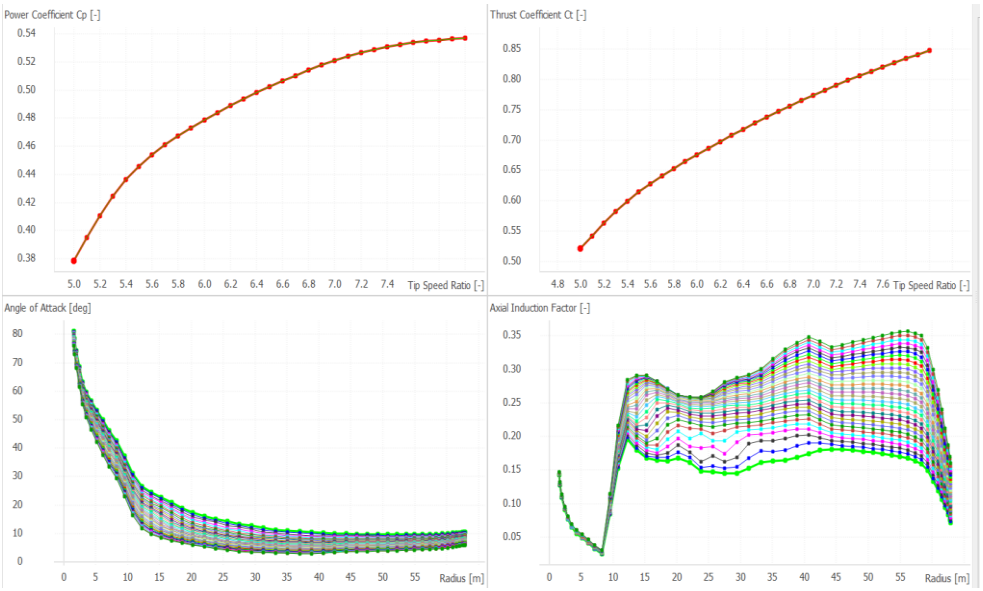

Fig. 11. Variation of power(L) and thrust(R) coefficients v/s TSR and AoA and axial induction factor v/s Radius

Characteristic BEM:

This BEM module uses cut in and cut out velocities as inputs along with pitch range of blade. Submodule simulations can be carried out over a specified range of windspeeds, rotational speeds and pitch angles. It is useful for designing control strategies for variable speed and pitch controlled turbines.

In this simulation it is observed at 8RPM, power developed is 8784kW is approached at 14.24 m/s, thrust is 927432 N and torque is 6.99MNm.

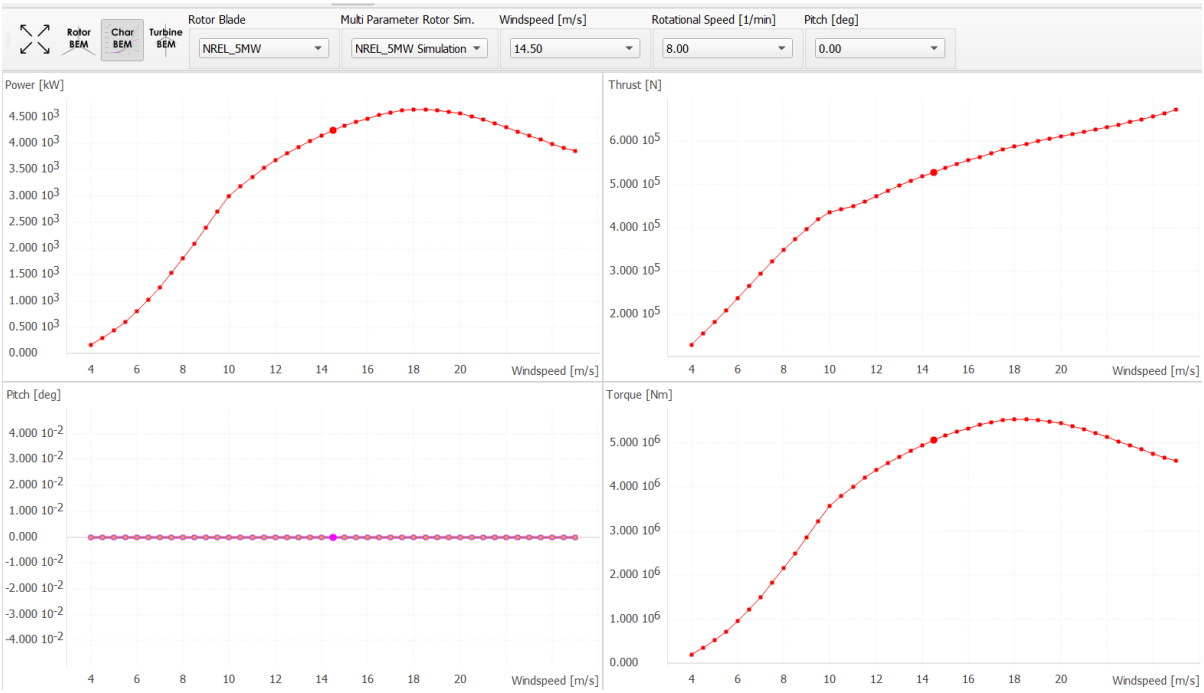

Turbine BEM:

This module is used to model steady state BEM simulations. Power regulation and Transmission can be setup according to user requirements. In our case, we went for a pitch limited output as we had specified a rated power as 5MW at which the blades pitch to maintain that power.

Transmission was selected as optimal where inputs are minimum and maximum rpm and TSR. Fixed losses can also be accounted for although this was not within the scope of this project. The outputs are the power curve, thrust and torque curves.

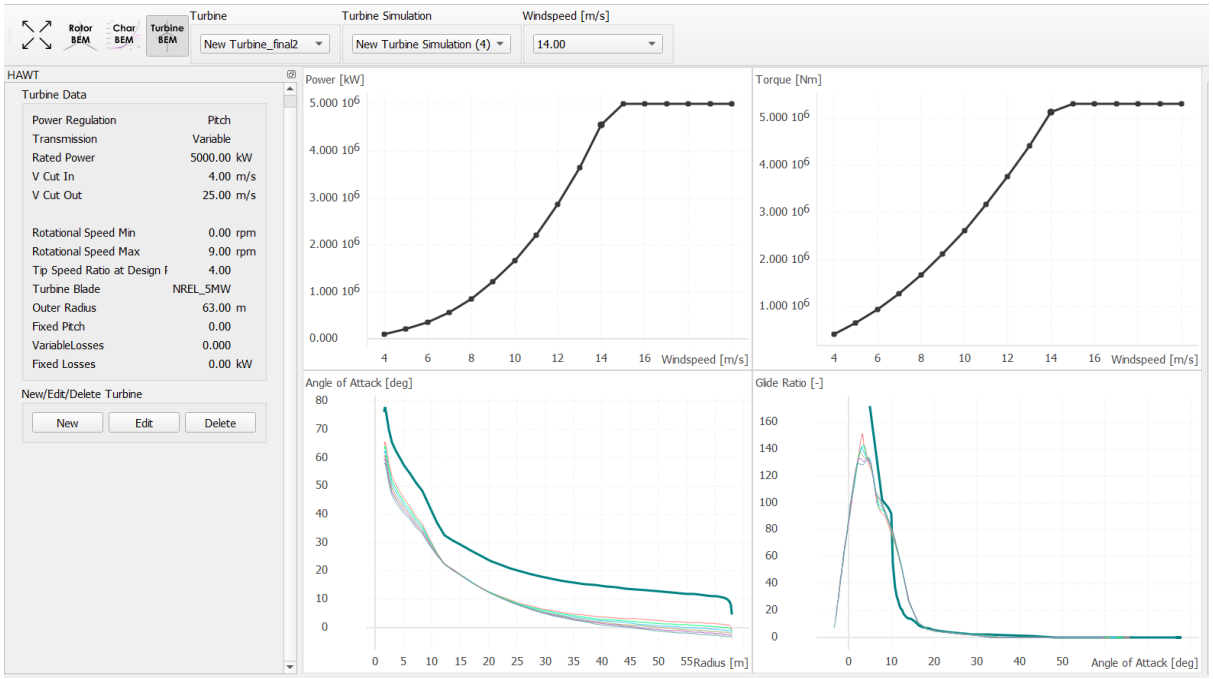

Turbine Definition Module:

Used to define turbine simulation taking into account mean velocity, max RPM and Tip speed ratio as well as wake types, and other aerodynamic effects such as the himmelskamp effect and tower shadow which in this case is not applicable as it only becomes relevant in a wind farm.

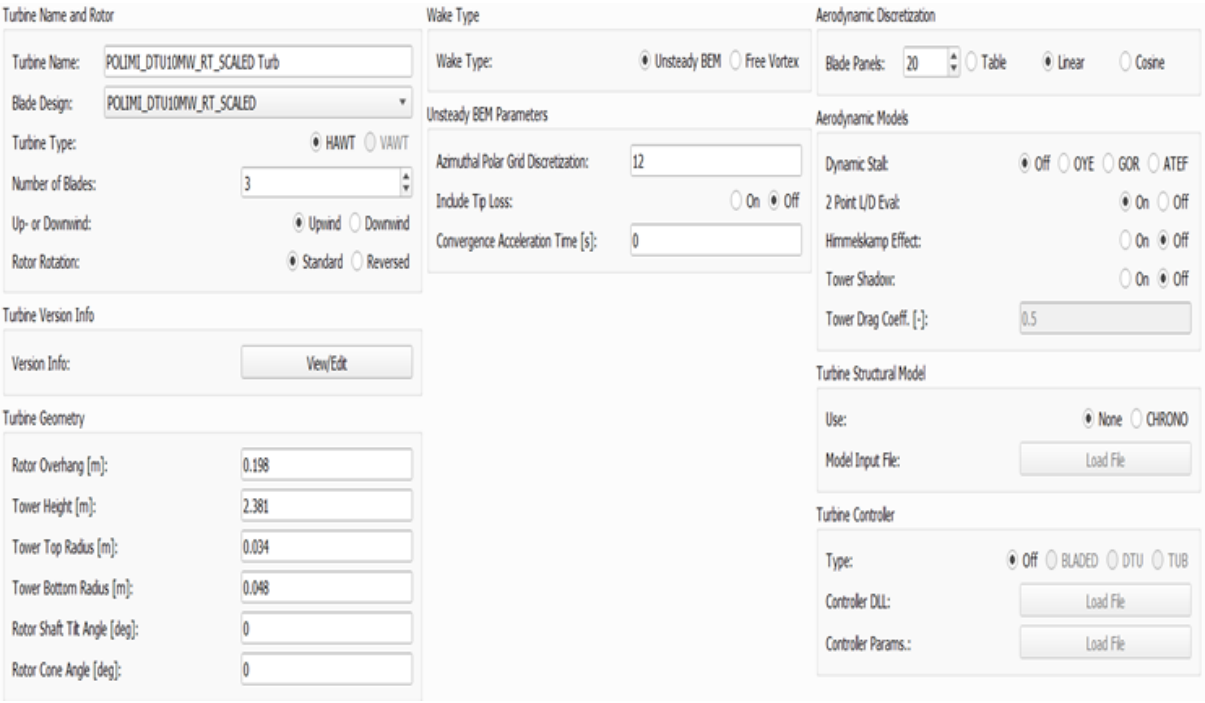

Turbine Simulation Module:

This module takes as input all the structural files, mean velocity, max rated RPM and water depth.

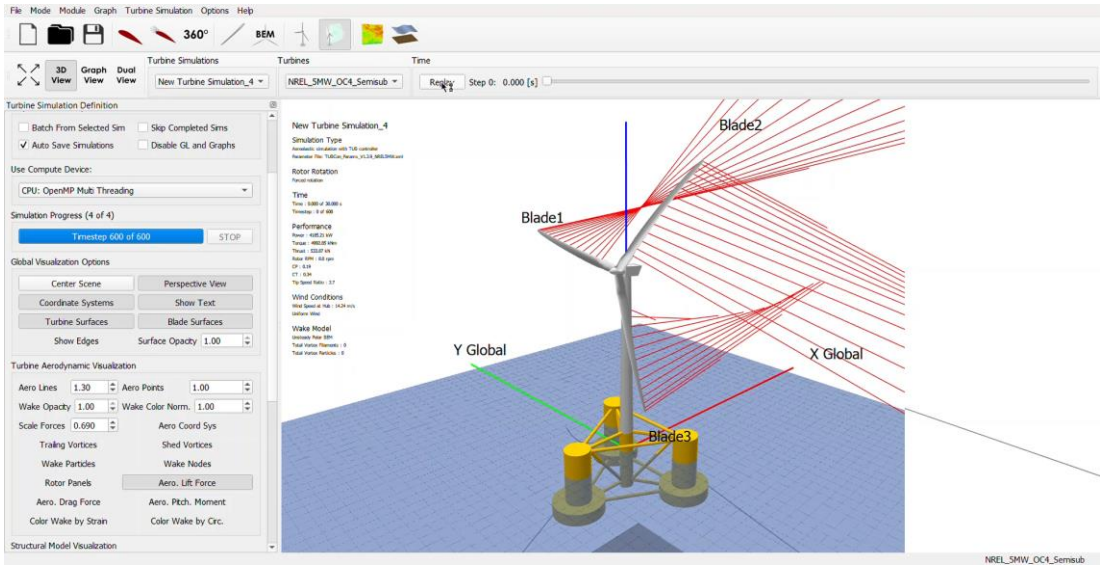

Power, Thrust and Torque graphs:

Windspeed [m/s]	Power [kW]	**Windspeed [m/s]**	**Thrust [N]**
4.00	-136.06	4.00	147841.53
4.50	-7.00	4.50	182691.28
5.00	154.59	5.00	219135.41
5.50	348.71	5.50	256220.08
6.00	576.78	6.00	294101.09
6.50	839.92	6.50	332710.41
7.00	1138.86	7.00	372072.78
7.50	1473.60	7.50	412035.50
8.00	1845.50	8.00	452622.53
8.50	2256.00	8.50	493726.41
9.00	2704.39	9.00	535415.13
9.50	3190.22	9.50	577434.63
10.00	3714.16	10.00	619840.19
10.50	4272.99	10.50	662228.31
11.00	4863.30	11.00	704003.69
11.50	5479.71	11.50	745231.63
12.00	6095.11	12.00	784549.56
12.50	6734.49	12.50	823096.25
13.00	7400.94	13.00	859633.44
13.50	8086.69	13.50	894535.38
14.00	8784.43	14.00	927432.81
14.50	9470.22	14.50	957429.38

Windspeed [m/s]	Torque [Nm]
4.00	-108270.06
4.50	-5567.43
5.00	123016.27
5.50	277491.75
6.00	458985.31
6.50	668385.19
7.00	906272.50
7.50	1172657.00
8.00	1468600.00
8.50	1795265.50
9.00	2152082.80
9.50	2538693.00
10.00	2955638.00
10.50	3400338.80
11.00	3870090.30
11.50	4360611.50
12.00	4850333.00
12.50	5359134.50
13.00	5889480.50
13.50	6435184.00
14.00	6990424.50
14.50	7536162.00

Conclusions:

i. Blade modelling using mean velocity of 14.24m/s retrieved from Morro Bay data done on QBlade. NA64_17, DU 25 and DU 21 profiles found to have the most optimal lift and pressure distributions.

ii. Stall from graphs is observed at AoA of 16^{o} at Cl 1.4 and Cd 0.03 for NA64_17

iii. Power curve shows it maxes out at 18m/s and 8RPM given a rated capacity of 5MW.

iv. Torque value is 699kNm at 14m/s and shows maximum value of 987kNM at 18m/s after which drag characteristics become predominant.

v. Thrust value for this particular turbine was found to be 981 kN at 14m/s and 1064kN at cut out velocity of 25m/s.

vi. We can conclude that the 5MW wind turbine can sufficiently generate power at the rated capacity for most of the time quite reliably

vii. It proves to be a good potential location for setting up a wind farm.

References

1. Definition of a 5-MW Reference Wind Turbine for Offshore System Development J. Jonkman, S. Butterfield, W. Musial, and G. Scott https://www.nrel.gov/docs/fy09osti/38060.pdf
2. CFD-based design load analysis of 5MW offshore wind turbine T. T. Tran, G. J. Ryu, Y. H. Kim, and D. H. Kim https://doi.org/10.2172/1882929
3. Airfoil family design for large offshore wind turbine blades B Méndez, X Munduate and U San Miguel https://iopscience.iop.org/article/10.1088/1742-6596/524/1/012022
4. Model Development and Loads Analysis of an Offshore Wind Turbine on a Tension Leg Platform, with a Comparison to Other Floating Turbine Concepts Denis Matha University of Colorado – Boulder Thesis Supervisors Jason Jonkman, Ph.D., NREL Tim Fischer, MSc Dipl.-Ing(FH), University Stuttgart, Germany https://doi.org/10.2172/973961
5. Chapter – 1,2 and 3: Offshore Wind Turbines Reliability, availability and maintenance- Peter Tavner.
6. Increasing Wind Turbine Tower Heights: Opportunities and Challenges
   Eric Lantz,1 Owen Roberts,1 Jake Nunemaker,1 Edgar DeMeo,2 Katherine Dykes,1 and George Scott1 https://doi.org/10.2172/1515397
7. Offshore Wind Energy Technical Potential for the Contiguous United States Anthony Lopez, Rebecca Green, Travis Williams, Eric Lantz, Grant Buster, and Billy Roberts https://doi.org/10.2172/1882929